M. Dehghani Firoozabadi, M. Shahbakhti, C.R. Koch, and S.A. Jazayeri. Thermodynamic control-oriented modeling of cycle-to-cycle exhaust gas temperature in an HCCI engine. *Applied Energy*, 110(0):236 – 243, 2013. ISSN 0306-2619. doi: 10.1016/j.apenergy.2013.04.055

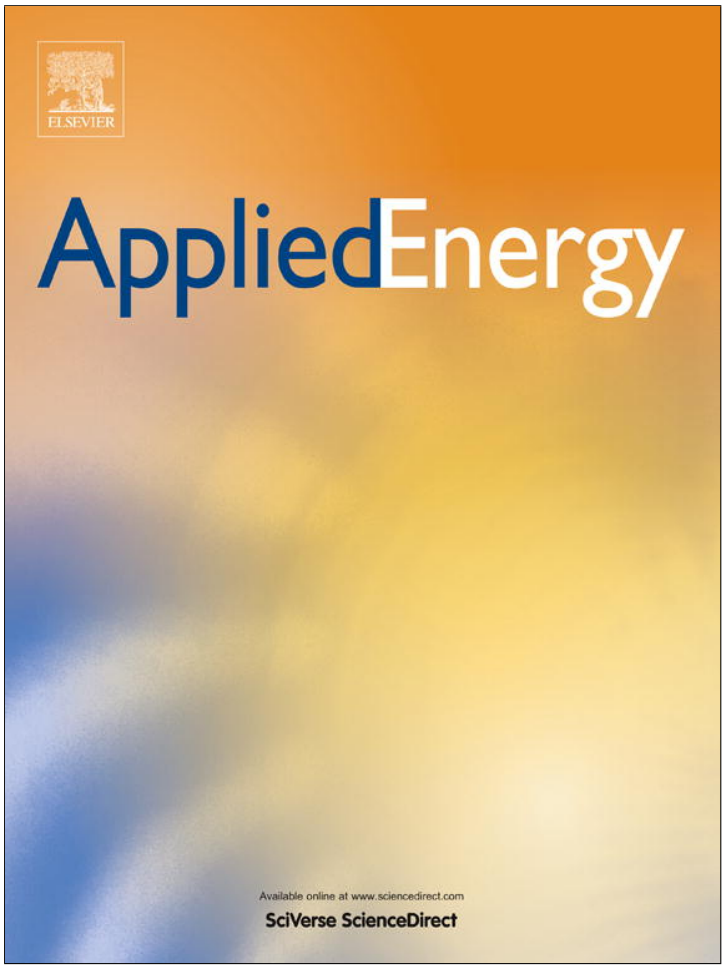

Applied Energy 110 (2013) 236–243

Contents lists available at SciVerse ScienceDirect

Applied Energy

journal homepage: www.elsevier.com/locate/apenergy

Thermodynamic control-oriented modeling of cycle-to-cycle exhaust gas temperature in an HCCI engine

M. Dehghani Firoozabadi [a], M. Shahbakhti [b,*], C.R. Koch [c], S.A. Jazayeri [a]

[a] Department of Mechanical Engineering, K.N. Toosi University of Technology, Tehran, Iran
[b] Mechanical Engineering-Engineering Mechanics Department, Michigan Technological University, Houghton, USA
[c] Department of Mechanical Engineering, University of Alberta, Edmonton, Canada

HIGHLIGHTS

- First thermodynamic model in the literature to predict exhaust temperature in HCCI engines.
- The model can be used for integrated control of HCCI combustion and exhaust temperature.
- The model is experimentally validated at over 300 steady state and transient conditions.
- Results show a good agreement between predicted and measured exhaust temperatures.
- Sensitivity of exhaust gas temperature to variation of engine variables is shown.

ARTICLE INFO

Article history:
Received 5 October 2012
Received in revised form 14 February 2013
Accepted 15 April 2013

Keywords:
HCCI
Exhaust gas temperature
Cycle-to-cycle simulation
Emission control

ABSTRACT

Model-based control of Homogenous Charge Compression Ignition (HCCI) engine exhaust temperature is a viable solution to optimize efficiency of both engine and the exhaust aftertreatment system. Low exhaust temperature in HCCI engines can limit the abatement of hydrocarbon (HC) and carbon monoxide (CO) emissions in an exhaust aftertreatment system. A physical–empirical model is described for control of exhaust temperature in HCCI engines. This model captures cycle-to-cycle dynamics affecting exhaust temperature and is based on thermodynamic relations and semi-empirical correlations. It incorporates intake and exhaust gas flow dynamics, residual gas mixing, and fuel burn rate and is validated with experimental data from a single cylinder engine at over 300 steady state and transient conditions. The validation results indicate a good agreement between predicted and measured exhaust gas temperature.

1. Introduction

HCCI engines offer diesel-engine like thermal efficiency with ultra-low nitrogen oxides (NOx) and negligible particulate matter emissions. Results in [1] show that an HCCI engine can obtain up to 35% lower brake specific fuel consumption rate and a 99% reduction in NOx compared to a conventional Spark Ignition (SI) engine. However, HCCI engines suffer from high unburned hydrocarbon and carbon monoxide emissions. In addition, low exhaust gas temperature in HCCI engines limits the conversion efficiency of the oxidation catalyst in the exhaust aftertreatment system. HCCI engines can have exhaust gas temperature as low as 120 °C [2] resulting in significant amounts of HC and CO tailpipe emissions. These emissions limit the practical operating range of HCCI engines.

Proper thermal control of the engine is essential to create desirable in-cylinder conditions in HCCI engines [3,4]. Combined control of combustion phasing and exhaust gas temperature is required to reduce high HC and CO emission in HCCI engines. This combined control requires an understanding of the physical phenomena affecting both HCCI combustion and exhaust temperature (T_{exh}). Several studies [5–7] have been done to estimate temperature of trapped residual gasses in HCCI engines, but very few studies have been done to predict exhaust temperature in HCCI engines. In [8], an empirical correlation is proposed to predict T_{exh} in HCCI engines. They found T_{exh} is highly dependent on specific energy of the input fuel and the crank angle of 50% mass fraction burned fuel. An approximate relation for predicting HCCI steady state exhaust

Abbreviations: aTDC, after top dead center; AFR, air fuel ratio; CAD, crank angle degree; CA50, crank angle for 50% burnt fuel; CO, carbon monoxide; EGR, exhaust gas recirculation; EGM, exhaust gas model; EOC, end of combustion; EVC, exhaust valve closing; EVO, exhaust valve opening; HC, hydrocarbons; HCCI, homogeneous charge compression ignition; IMEP, indicated mean effective pressure; IVC, intake valve closing; IVO, intake valve opening; MKIM, modified knock integral model; NASA, national aeronautics & space administration; NOx, oxides of nitrogen; ON, octane number; PM, particulate matter; PRF, primary reference fuel; P, products; R, reactants; SI, spark ignition; SOC, start of combustion; TDC, top dead center.

* Corresponding author.
E-mail address: mahdish@mtu.edu (M. Shahbakhti).

0306-2619/$ - see front matter © 2013 Elsevier Ltd. All rights reserved.
http://dx.doi.org/10.1016/j.apenergy.2013.04.055

Nomenclature

A	area (m^2)
CA_X	crank angle for X% burnt fuel (CAD aTDC)
C_v	constant-volume specific heat capacity $\left(\frac{kJ}{kg\,K}\right)$
C_p	constant-pressure specific heat capacity $\left(\frac{kJ}{kg\,K}\right)$
C_R	compression ratio (–)
CoC	completeness of combustion (–)
EGR	fraction of exhaust gas recirculated (–)
h_c	convective heat transfer coefficient $\left(\frac{W}{m^2\,K}\right)$
L	Instantaneous cylinder height (m)
LHV	lower heating value of fuel $\left(\frac{kJ}{kg}\right)$
m	mass (kg)
N	engine speed (rpm)
Φ	equivalence ratio (–)
P	pressure (kPa)
Q	heat (kJ)
S_p	piston speed $\left(\frac{m}{s}\right)$
t	time (s)
T	temperature (K)
θ	crank angle (CAD)
U	internal energy (kJ)
V	volume (m^3)
W	work (kJ)
X_r	residual gas mass fraction (–)
X_d	mixture dilution fraction (–)
y	mass fraction (–)

Subscripts

a	air
ce	flow from cylinder to exhaust
ch	charge (air + fuel + EGR)
$cool$	coolant
dis	displacement
ec	flow from exhaust to cylinder
exh	exhaust
egr	exhaust gas recirculated
eoc	end of combustion
evc	exhaust valve closing
evo	exhaust valve opening
f	fuel
g	cylinder gas
iso	isooctane
ivc	intake valve closing
ivo	intake valve opening
m	intake manifold
r	residual gas
soc	start of combustion
t	total gas
w	cylinder walls

gas temperature as a function of gas temperature at intake valve closing is developed in [9]. Heat losses and work effects are ignored and T_{exh} is considered to be equal to the residual gas temperature at the end of exhaust stroke [9]. A physical model for predicting HCCI exhaust gas temperatures is the focus of this paper and is, to the authors' knowledge, the first control-oriented physical modeling of the cycle-to-cycle exhaust temperature in HCCI engines. Although the focus of this work is on predicting T_{exh}, the full cycle model can be also used to predict combustion phasing and output power in HCCI engines.

The remainder of this paper is organized in sections. Section 2 develops a thermodynamic model to predict cycle-to-cycle T_{exh} for an HCCI engine. The resulting model is experimentally validated using both steady-state and transient operating data in Section 3. The sensitivity of T_{exh} from varying three main engine variables (intake manifold pressure, octane number and equivalence ratio) is investigated in Section 4. The last section is a summary.

2. Model description

An HCCI engine cycle is sub-divided into the following sequence of valve events: intake stroke, compression stroke, combustion and expansion stroke and exhaust stroke. The complete HCCI engine cycle simulation model consists of these interlinked components which are then used to predict T_{exh}.

2.1. Intake stroke

2.1.1. IVC temperature and pressure

The thermodynamic state (including temperature, pressure and species concentration) of the cylinder charge at intake valve closing (IVC) moment strongly influences the ignition timing and consequently T_{exh} of HCCI engines. The time history, including heat transfer to the cylinder walls and rate of change of the thermodynamic state, also influence the subsequent ignition timing. The temperature of the air–fuel mixture at IVC (T_{ivc}) is a dominant factor controlling chemical reaction rates leading to auto-ignition [10]. Intake valve closing pressure (P_{ivc}) affects the rate of oxygen reaction with fuel by changing the concentration of the blend [11]. To predict T_{ivc}, the first law of thermodynamics is applied between IVO and IVC. A quasi-steady assumption is used and the properties of the gas are assumed constant and homogeneous. Furthermore, the changes in kinetic and potential energy of the gas are ignored. Using these assumptions, the first law of thermodynamics for in-cylinder gas as an open control volume is:

$$T_{ivc} = (1 - X_r)\frac{C_{p,man}}{C_{v,ivc}}T_{man} + X_r\frac{C_{v,r}}{C_{v,ivc}}T_r + \frac{(Q - W)_{c.v}}{C_{v,ivc}\,m_t} \tag{1}$$

T is the temperature where the subscript of ivc, man and r denote intake valve closing, intake manifold and residual gas respectively. $C_{p,man}$ is the constant-pressure specific heat capacity of intake charge and C_v is the constant-volume specific heat capacity of in-cylinder gas. C_p and C_v are determined by using NASA polynomials [12].

W is the amount of work which it is done during the intake stroke. In-cylinder volume changes, to calculate work, is determined by a slider-crank mechanism [13].

The residual gas mass fraction, X_r, is determined by the following equations:

$$X_r = \frac{m_r}{m_t} \tag{2}$$

$$m_t = m_a + m_{egr} + m_f + m_r \tag{3}$$

where m indicates the mass and the subscripts a, egr, f, r and t denote air, exhaust gas recirculation, fuel, residual gas and total respectively. These are all calculated at *IVC* except m_r which is calculated at the *EVC* moment.

The heat transfer to the cylinder walls is modeled using the modified Woschni heat transfer correlation adopted for HCCI engines [14]:

$$Q = -h_c A_s (T_g - T_w) \tag{4}$$

where A_s is in-cylinder surface area, T_g and T_w are in-cylinder gas temperature and average wall temperature respectively. The convective heat transfer coefficient, h_c, is given by:

$$h_c(t) = \alpha_s L(t)^{-0.2} P(t)^{0.8} T(t)^{-0.73} (c_1\ \bar{S}_p)^{0.8} \tag{5}$$

where L, P and T are the cylinder height, the gas pressure and the temperature (all varying with the time). $\bar{S}_p$ is the average piston speed and α_s is the scaling factor that is used to tune the correlation to match a specific engine geometry [14]. The value of $\alpha_s = 2$ is chosen using the simulation results from [15]. The value of c_1 is 6.18 for intake and exhaust strokes and 2.28 for other strokes [14].

The intake valve closing pressure (P_{ivc}) is calculated using the ideal gas law and assuming that the air–fuel blend is an ideal gas.

2.1.2. Valves mass flow rate model

The mass flow rate through the intake and exhaust valves is modeled as one-dimensional, steady-state, compressible, isentropic flow by using the orifice equation [13].

The diameter of the valves are 32 mm and 27 mm for intake and exhaust valves respectively and the valve lift, measured off-line, is shown in Fig. 1 for both the intake and exhaust valves.

2.1.3. Residual gas model (initial value estimation)

Trapped exhaust gas and back-flow of the exhaust gas into the cylinder during the valve overlap period are the main sources of residual gas in HCCI engines. Residual gas from the previous cycles has a significant effect on mixture conditions at IVC of the current cycle. Residual gas affects temperature, composition and dilution level of the mixture. These effects cause coupling dynamics between successive HCCI engine cycles. The residual gas mass fraction (X_r) depends mainly on valve timing, fuel amount, engine speed, intake and exhaust manifold pressure [17]. Here, an initial value of (X_r) is estimated using a model [18]:

$$X_r = \frac{r_c - 1}{r_c} \Phi \frac{V_{ivo}}{V_{dis}} \left(\frac{P_{exh}}{P_m}\right)^{\frac{1}{k}} \left(1 + \frac{LHV}{c_v\ T_m \left(\frac{m_t}{m_f}\right) r_c^{k-1}}\right)^{\frac{-1}{k}} \tag{6}$$

where r_c is the compression ratio, P_{exh} is the exhaust pressure and k is the ratio of specific heat capacities. V_{ivo} is the cylinder volume at IVO and V_{dis} is the displacement volume. LHV stands for the lower heating value of the fuel and c_v is the constant-volume specific heat capacity of the in-cylinder gas at IVC. Eq. (6) only provides an initial estimate for X_r and the final value of X_r is calculated in an iterative process using Eq. (2).

The temperature and amount of EGR influence T_{ivc} and the specific heat capacity of in-cylinder mixture. The EGR dilution effect reduces chemical reactivity of the mixture and retards ignition timing by replacing oxygen with inert chemical species [19]. A mixture dilution fraction (X_d) is defined to account for the dilution caused by both external EGR and the residual gases (internal EGR) [16]:

$$X_d = EGR + \frac{X_r}{1 - X_r} \tag{7}$$

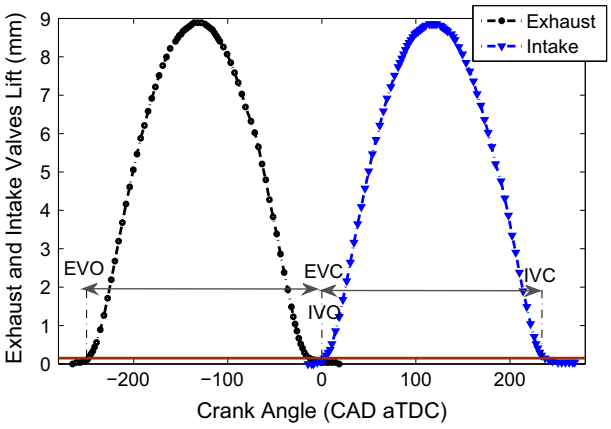

Fig. 1. Measured lift profile for valves of Rover K7 cylinder head. [The solid horizontal line shows the defined threshold (0.15 mm) for opening/closing point of valves.].

2.2. Compression stroke

2.2.1. Isentropic compression

Compression of the unburned mixture prior to combustion can be accurately estimated with a polytropic relation ($PV^k = c$) [13]. Here blow-by is assumed zero and a polytropic relation is applied to calculate the temperature and pressure of the mixture at the start of combustion (SOC). A blow-by model should be added if the HCCI engine has a high blow-by rate since the significant blow-by can have a major error in T_{exh} and so then needs to be modeled in that case. In this study, the engine has low amounts of blow-by so this is neglected. The constant $k = 1.32$, for the average specific heat capacity ratio of the mixture, is a best fit from a thermo-kinetic model on simulated compression results [20] for the PRF[1] blends used in this study.

2.2.2. SOC (Auto-ignition) model

HCCI combustion has similar chemical kinetics to that of knock (premature auto-ignition) in SI engines [21]. A modified knock integral model (MKIM) [20] is used to predict the crank angle of start of combustion (θ_{SOC}):

$$\int_{\theta_{ivc}}^{\theta_{soc}} \frac{\Phi^B}{A \exp\left(\frac{C\ (P_{ivc}\ v_c^{k_c})^D}{T_{ivc}\ v_c^{k_c-1}}\right) N} d\theta = 1.0 \tag{8}$$

where θ is the engine crank angle and B, C and D are constant parameters. The values of v_c and A are determined by:

$$v_c(\theta) = \frac{V_{ivc}}{V(\theta)}, \quad A = E_1\ X_d + E_2 \tag{9}$$

where E_1 and E_2 are constant parameters. The constant parameters values are taken from [16] for the Ricardo single cylinder engine.

2.3. Combustion period

2.3.1. Fuel burn rate model

Combustion duration is one of the main factors affecting the exhaust temperature in HCCI engines [22]. A Wiebe function [23] is modified to predict burned fuel mass fraction (x_b) and combustion duration θ_d as [24]:

$$x_b(\theta) = 1 - exp\left[-2.02\left(\frac{\theta - \theta_{soc}}{\theta_d}\right)^{5.08}\right] \tag{10}$$

$$\theta_d = 5.98\ (1 + X_d)^{0.01}\ \Phi^{-0.02} \tag{11}$$

where θ_{soc} and θ_d are SOC crank angle and combustion duration in

[1] PRF number is the iso-Octane volume percentage in the mixture of n-Heptane fuel (PRF0) and iso-Octane fuel (PRF100).

CAD respectively. This model is an empirical relation which has been determined and verified with the experimental data. The model predicts CA50 with less than 2 CAD error [24]. These are then used to calculate the crank angle at the End of Combustion (*EOC*) as: θ_{eoc} = CA99. θ_{eoc} is defined as the crank angle where 99% mass fraction of fuel has been burned. The model parameters are determined by applying Nelder–Mead simplex minimization method [16].

2.3.2. EOC state equations

The combustion chamber is considered as a single zone closed system and the blow-by is assumed to be zero. The first law of thermodynamics applied between SOC and EOC is used to calculate temperature and pressure of in-cylinder gas at EOC as:

$$U_{eoc} = U_{soc} + Q_{fuel} - Q_w - W_{soc-eoc} \tag{12}$$

where U denotes the internal energy, Q_{fuel} is the released energy from burning the fuel, Q_w is the heat loss from the in-cylinder gas to the walls, and $W_{soc\text{-}eoc}$ is the generated work during SOC–EOC. Q_w is ignored for two reasons. First, the heat transfer area is small since a desirable HCCI combustion occurs at a crank angle close to TDC [25]. Second, the duration of HCCI combustion is short thus the time available for heat transfer is small. $W_{soc\text{-}eoc}$ is determined using the following empirical correlation [16]:

$$W_{soc-eoc} = m_f LHV \times \overbrace{\frac{P_m^{2.629} N^{-2.860}}{(1+EGR)^{-0.056}} \left(0.021\ \theta_{soc}^2 - 3.711\ \theta_{soc} + 0.010\right)}^{\mathbb{W}} \tag{13}$$

where m_f is the mass of injected fuel per cycle.

The released energy from the fuel is:

$$Q_{fuel} = m_f\ CoC\ LHV \tag{14}$$

CoC is the completeness of combustion and is calculated from an empirical correlation [16]:

$$CoC = \frac{\Phi^{0.169} P_m^{0.165}}{(1+EGR)^{0.053}} \left(-0.001\ \theta_{soc}^2 + 0.458\ \theta_{soc} + 1.390\right) \tag{15}$$

CoC as a function of SOC and equivalence ratio is shown in Fig. 2. A lower *CoC* is observed in Fig. 2 for early and lean ignition conditions. In addition, the results in Fig. 2 show HCCI lean burn combustion has high *CoC* ranging from 85% to 98%, compared to typical SI engines.

Eqs. (12) and (13) are combined to determine in-cylinder gas temperature at EOC (T_{eoc}) [16]:

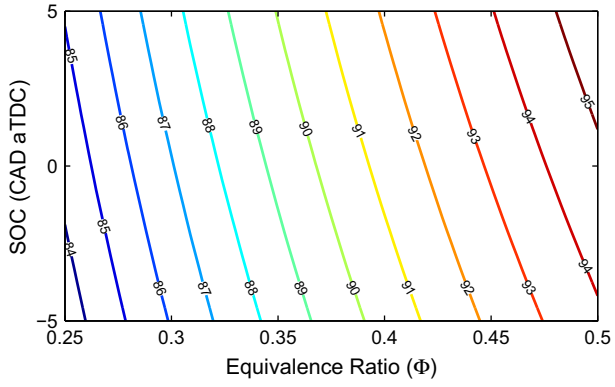

Fig. 2. Simulated CoC values for a range of SOCs and equivalence ratios. (P_{man} = 100 kPa and EGR = 30%).

$$T_{eoc} = \frac{\left(\sum_i c_{v,i} y_i\right)_R T_{soc} + \frac{m_f}{m_t} LHV(CoC - \mathbb{W})}{\left(\sum_i c_{v,i} y_i\right)_P} \tag{16}$$

where y indicates the mass fraction of each combustion products (P) and reactants (R). To calculate mass fraction of combustion products, a general reaction equation of the fuel blend for complete lean combustion is used as detailed in [26].

To calculate the pressure at EOC (P_{eoc}), the ideal gas state equation for the air–fuel mixture at EOC and IVC is used.

2.4. Expansion stroke

2.4.1. Polytropic expansion

Temperature and pressure of the burned gasses at EVO are found using a polytropic relation [16].

2.5. Exhaust stroke

2.5.1. Single zone model

The properties for the gases entering and exiting the cylinder are assumed steady and homogeneous resulting in a quasi-steady state assumption. Using the first law of thermodynamics for the exhaust gas, with an open control volume between the EVO and EVC yields [16]:

$$T_{evc} = \frac{T_{evo}\left(\sum_i m_{i,evo} c_{v_i,evo} - \sum_i c_{p_i,evo}(m_{i,ce} + m_{i,ec})\right) + Q_w + P_{evo}\ dV}{\sum_i m_{i,evc} c_{v_i,evc}} \tag{17}$$

Q_w is the heat transfer to the cylinder wall and it is determined using the similar approach to Section 2.1.1. The indexes of *ec* and *ce* refer to back flow from the exhaust manifold to the cylinder and the exhaust flow from the cylinder to the exhaust manifold respectively. Since this engine is configured with no valve overlap, no flow between the intake manifold and the cylinder is considered during the exhaust stroke.

2.5.2. Residual gas state

Once the exhaust valves are closed some of burnt gases are trapped inside the cylinder. These residual gases affect the combustion for the next cycle. The temperature (T_r) and mass fraction of residual gas (X_r) are determined based on in-cylinder gas properties at EVC.

2.5.3. Exhaust Gas Model (EGM)

Gas temperature entering into the exhaust port varies from T_{evo} to T_{evc}. The exhaust port inlet temperature is assumed to be the average of T_{evo} and T_{evc}.

$$T_{g,in} = \frac{T_{evo} + T_{evc}}{2} \tag{18}$$

The exhaust port is considered as a control volume with no boundary work: $W_{c.v.} = 0$

A quasi-steady assumption is used and the properties of gas are taken as constant and homogeneous. In addition, the change in kinetic and potential energy of the exhaust gases are ignored. The exhaust gas temperature (T_{exh}) is calculated using the first law of thermodynamics:

$$T_{exh} = T_{g,in} + \frac{Q_{c.v.}}{m_t(1 - X_r)c_p} \tag{19}$$

where $Q_{c.v.}$ is the convective heat transfer between exhaust gases and the exhaust port walls:

$$Q_{c.v.} = -h_c A(T_g - T_w) \tag{20}$$

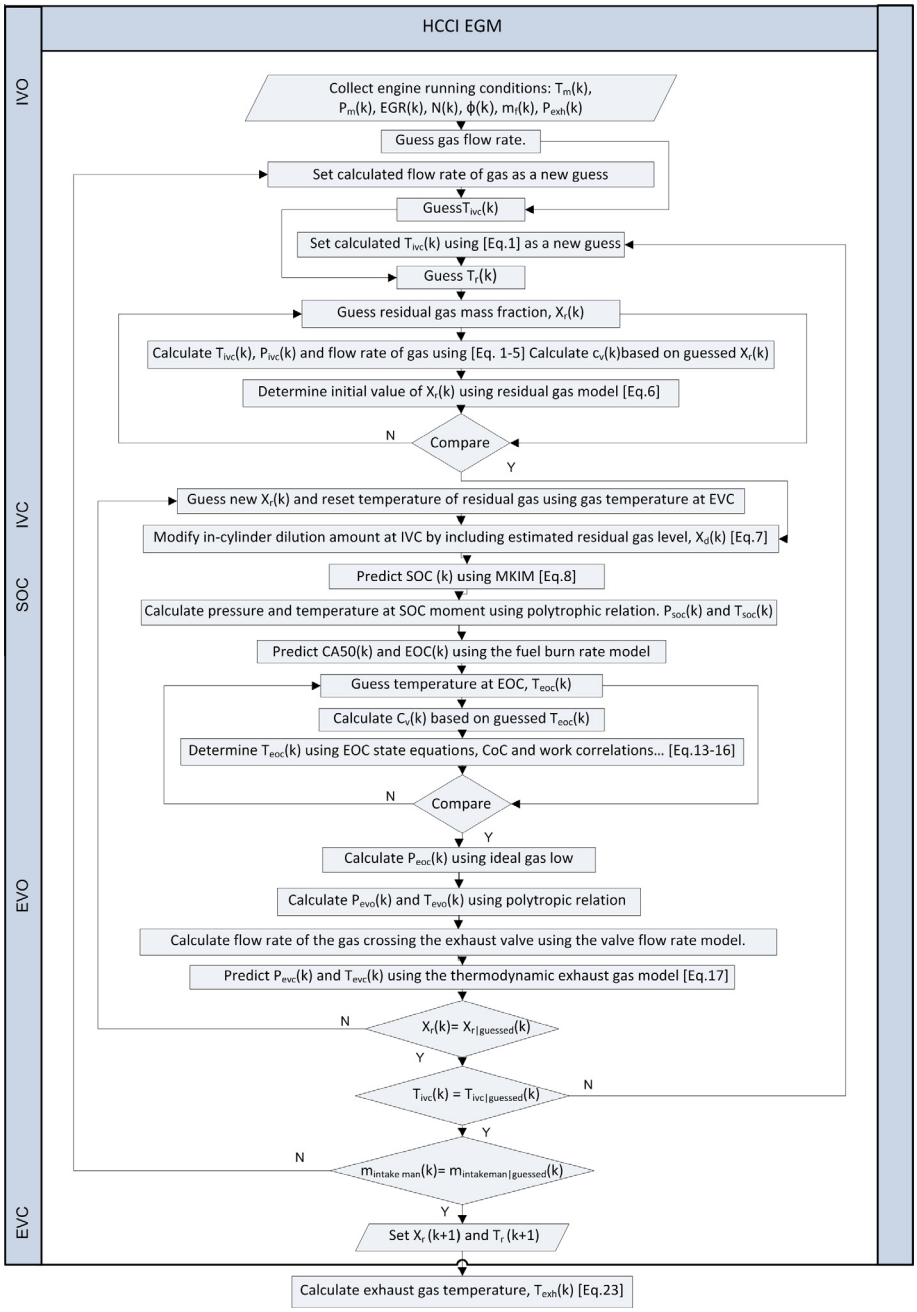

Fig. 3. Flowchart of HCCI EGM.

and T_g is the average temperature of the gases inside the exhaust port. T_g is assumed to be the average of the gas temperatures between the inlet of exhaust port ($T_{g,in}$) and the outlet (T_{exh}) of exhaust port:

$$T_g = \frac{T_{g,in} + T_{exh}}{2}. \tag{21}$$

The variable A in Eq. (20) is the heat transfer surface area and is:

$$A = \pi d_p l_p \tag{22}$$

where d_p is the exhaust port diameter and l_p is the exhaust port length. Solving for T_{exh} by substituting Eqs. (20)–(22) into Eq. (19) results in:

$$T_{exh} = \frac{T_{evo} + T_{evc}}{2}\left[\frac{2m_t(1-X_r)c_p - h_c\,A}{2m_t(1-X_r)c_p + h_c\,A}\right] + \frac{2h_c\,A}{2m_t(1-X_r)c_p + h_c\,A}T_w. \tag{23}$$

2.6. HCCI Exhaust Gas Model configuration

Combining all the sub-models results in a thermodynamic model of an HCCI engine which can be used to predict cycle-to-cycle exhaust temperature. The inter-relation of the sub-models of the complete HCCI Exhaust Gas Model (HCCI EGM) is shown as a flowchart in Fig. 3. The HCCI EGM requires these seven inputs: engine speed, equivalence ratio, EGR, mass of injected fuel, exhaust port

pressure, intake manifold temperature and pressure. All these inputs can be easily measured or estimated on a real engine. In addition to T_{exh}, the HCCI EGM calculates combustion metrics such as SOC and CA50. Thus the model can be used to control both T_{exh} and combustion phasing in HCCI engines.

3. Experimental validation and discussion

Steady state and transient experimental data are used to evaluate the performance of the HCCI EGM. Experimental data are taken from a Ricardo single-cylinder engine with specifications listed in Table 1.

3.1. Steady state operation

The engine is run at 304 different steady state operating conditions which are listed in Table 2. These operating conditions cover an extensive HCCI operation range with the Ricardo single cylinder engine. The compression ratio of the engine is low (i.e. $C_R = 10$), limiting the HCCI operation to occur only for lower octane number fuels and at lower engine speeds. PRF40 for the Ricardo engine is the highest PRF for which HCCI operation is possible for a range of engine loads. High cyclic variation (misfire) limits the operating range of the HCCI engine at low load and knocking limits the operating range at high load. A pressure rise rate of 7 bar/CAD was defined as the threshold for the knock limit and COV_{IMEP} of 5% was defined as the misfire (combustion stability) limit.

A comparison of the simulated T_{exh} with the experimentally measured T_{exh} at 304 steady state operating conditions is shown in Fig. 4. The simulation time for each engine cycle is 0.3 s on a 2.66 GHz Intel® Core™ 2 Duo processor. The HCCI EGM predicts T_{exh} with average and standard deviation errors of 21 °C and 17 °C respectively that is acceptable for exhaust aftertreatment modeling since T_{exh} ranges within 250–400 °C and 21 °C is a 5–8% relative error. In addition, the HCCI EGM can be used for HCCI combustion control since this engine has low residual gas fraction (~7%), thus the T_{exh} error of 21 °C will not cause a substantial error on residual gas temperature and consequently cause insignificant error on T_{ivc} and subsequent combustion timing. However, since the HCCI EGM assumes constant cylinder wall temperature the T_{exh} prediction from the HCCI EGM could be further improved if variation in wall temperature as a function of coolant temperature and engine load were augmented to the model [4]. Those operating points with large T_{exh} prediction error in Fig. 4 are the points with coolant temperature below engine fully warmed up operation (i.e. 82–84 °C).

Table 1
Ricardo single-cylinder engine specifications.

Parameters	Values
Bore × stroke (mm)	80 × 88.9
Displacement (l)	0.447
Compression ratio (–)	10
Number of valves (–)	4
IVO, IVC (CAD aTDC)	5, 235
EVO, EVC (CAD aTDC)	−250, 5

Table 2
Measured operating conditions of 304 steady-state data points used in this study.

Variables	Values
Fuel, PRF (–)	0–40
Engine speed, N (rpm)	800–1340
Intake manifold temperature, T_m (°C)	59–162
Equivalence ratio, ϕ (–)	0.29–0.83
Intake manifold pressure, P_m (kPa)	88–161
EGR (%)	0–30
Coolant temperature, T_{cool} (°C)	41–84

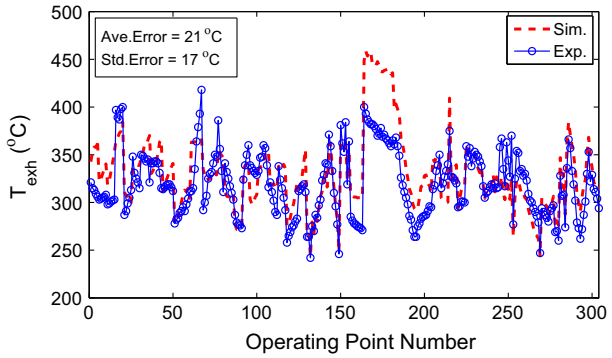

Fig. 4. Comparison between simulated and experimental T_{exh} for four PRF blends at a range of steady-state engine conditions listed in Table 2.

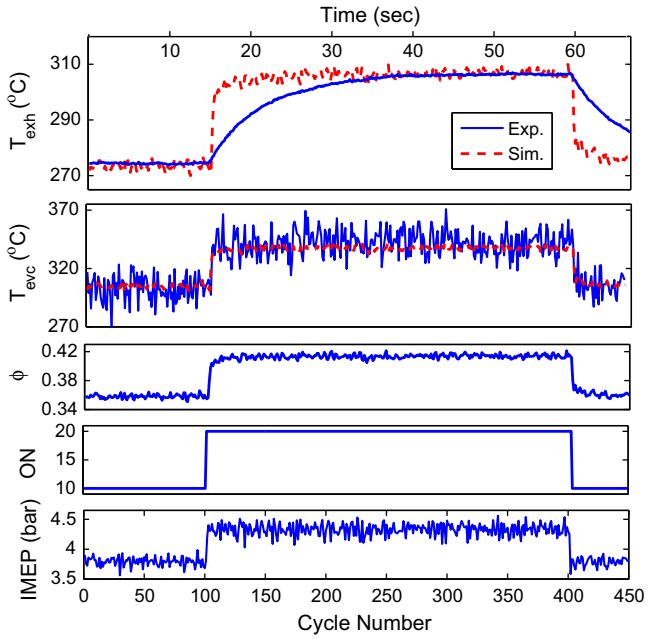

Fig. 5. Comparison between HCCI EGM simulated and experimental T_{exh} for a transient fueling operation in fully warmed up engine condition – no thermocouple measurement dynamics.

3.2. Transient operation

The HCCI EGM output is now compared to experimental data for transient conditions. Fig. 5 compares HCCI EGM simulated output and experimental T_{evc} and T_{exh} for a transient fueling operation. For the 450 engine cycles, the average and standard deviation errors between the exhaust gas temperature measurement and model prediction are 5 °C and 6 °C respectively. It is interesting to note that a large difference between simulated and experimental exhaust gas temperature is observed right after a step change in engine fueling. This difference is attributed to the response speed of the exhaust temperature thermocouple which takes some time to respond to a step change in T_{exh}.

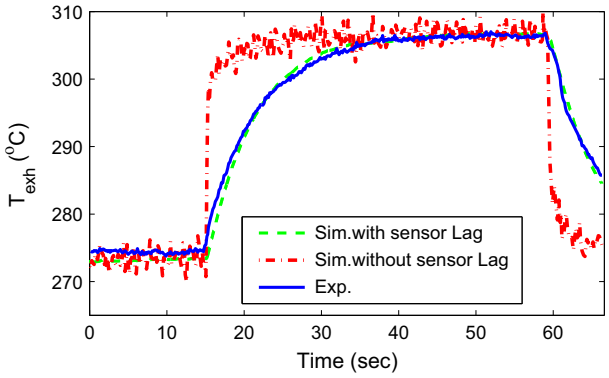

Fig. 6. Comparison between experimental and simulated T_{exh} – including the thermocouple measurement dynamics.

3.3. Sensor dynamics – thermocouple lag effect

To compensate for the dynamics of the thermocouple that measures T_{exh}, a first order model is proposed. A 1/32″ sheathed J-type thermocouple is used for the exhaust temperature measurement. The response time of the thermocouple limits how fast it can respond to an instantaneous step change in temperature. The dynamic response of the thermocouple is modeled as a first order lag element with a time constant of τ:

$$G(s) = \frac{k_p}{\tau s + 1} \tag{24}$$

System identification is used to find k_p and τ for the thermocouple and results in $\tau = 2.052$ s, $k_p = 1.00$. Incorporating the thermocouple dynamics in the HCCI EGM results in simulated T_{exh} with sensor lag and is shown in Fig. 6. As shown in Fig. 6 the simulated T_{exh} is now in good agreement with experimental data with average and standard deviation errors less than 5 °C.

4. Influence of operating conditions on T_{exh}

Three factors that influence T_{exh} in HCCI engines are: intake pressure, fuel octane number and fuel equivalence ratio [8]. The influence of these three factors on T_{exh} is shown in Fig. 7 by using the HCCI EGM parameterized for this engine. The operation conditions chosen for the simulation in Fig. 7 are in the middle of the engine operating conditions listed in Table 2.

These simulation results allow the sensitivity of T_{exh} to the three factors to be examined at a nominal operating point. Results in Fig. 7a indicate T_{exh} decreases when the intake pressure increases. This is mainly caused by advancing the HCCI combustion when the intake pressure is increased [8]. When the ignition is delayed, most of the energy is released partway down the expansion stroke and this increases the exhaust gas temperature. Results in Fig. 7b show T_{exh} increases when the fuel octane number increases. Increasing fuel octane number leads to a delayed auto-ignition which results in hotter exhaust gases. In addition, the combustion duration is prolonged with increasing fuel octane. Delayed and prolonged combustion results in hotter exhaust gases. The variation in T_{exh} versus the fuel equivalence ratio (Φ) is shown in Fig. 7c. It is observed that richer fuel–air mixtures (i.e. higher Φ) lead to higher T_{exh} despite the fact that HCCI auto-ignition occurs earlier at higher Φ. This is mainly due to higher injected fuel energy content at higher Φ. More combustion energy is released when the fuel mass flow rate in the intake charge increases at higher equivalence ratio operating conditions. Approximating the sensitivity of T_{exh} to intake manifold pressure, octane number and equivalence ratio by using a linear slope in Fig. 7 results in −24 °C/bar, 50 °C/100ON and 400 °C/Φ respectively. Thus, it is clear that at this operating condition T_{exh} is most sensitive to equivalence ratio (Φ).

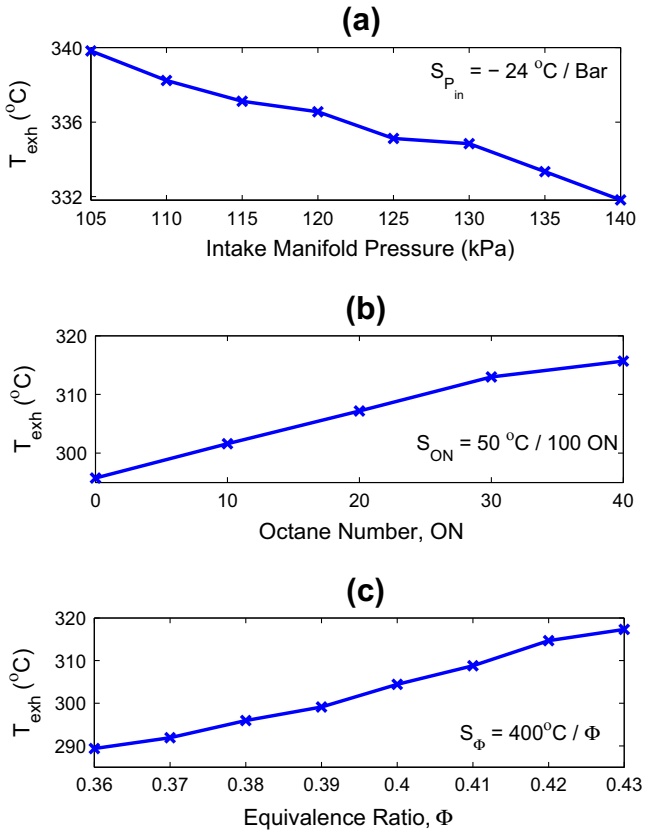

Fig. 7. Variations of simulated exhaust gas temperatures as a function of P_{man}, ON and Φ. S_x indicates linear sensitivity of T_{exh} to the variation of a parameter x. (a) $ON = 20$, $N = 1100$ rpm, $\Phi = 0.48$, $P_{man} = 105$–140 kPa, $T_{man} = 110$ °C, EGR = 15%, (b) $ON = 0$–40, $N = 1100$ rpm, $\Phi = 0.48$, $P_{man} = 125$ kPa, $T_{man} = 110$ °C, $EGR = 15\%$,(c) $ON = 20$, $N = 1100$ rpm, $\Phi = 0.36$–0.43, $P_{man} = 125$ kPa, $T_{man} = 110$ °C, $EGR = 15\%$.

5. Summary

A HCCI EGM full engine-cycle thermodynamic–empirical model is developed with outputs of T_{exh} and combustion timing of an HCCI engine. This model provides insight into the sensitivity of the outputs to the seven inputs and will be useful in developing HCCI combustion timing control strategies. The HCCI EGM is experimentally validated at 304 steady-state operating points and one transient operating condition. Over the entire experimental range the HCCI EGM predicts exhaust gas temperature T_{exh} with an average and standard deviation errors of 21 °C and 17 °C respectively.

Intake pressure, fuel octane number and fuel equivalence ratio substantially affect T_{exh} since these three variables can influence the onset and duration of HCCI combustion as well as the input energy content to the engine. Holding all other inputs constant, T_{exh} increases when: the fuel octane number is increased; the fuel equivalence ratio is increased; the intake pressure is decreased.

The HCCI EGM is also able to capture T_{exh} dynamics during a step change in fueling and is computationally efficient (0.3 s to simulate an engine cycle on a PC). To match transient experimental data with the simulation it is important to model the thermocouple sensor dynamics and a first order lag model of the thermocouple is found to be sufficient.

In future work the model could be further improved by modeling the wall temperature as a function of engine load and coolant

temperature. In addition, for engines with significant blow-by a model to include the blow-by gas flow is needed.

References

[1] Johansson B. Partially premixed combustion, PPC, for high fuel efficiency engine operation, SAE panel presentation (FFL225) on high efficiency IC engines. International powertrains, fuels and lubricants meeting; 2009. <http://www.sae.org/events/pfl/presentations/2009/BengtJohansson.pdf>.

[2] Williams S, Nakazono L, Hu Ohtsubo TH, Uchida M. Oxidation catalysts for natural gas engine operating under HCCI or SI conditions. SAE paper no. 2008-01-0807; 2008.

[3] Constandinides G, Dowty M. Modelling and experimental study of thermal management system for HCCI. SAE paper no. 2011-24-0160; 2011.

[4] Widd A, Tunestål P, Johansson R. Physical modeling and control of homogeneous charge compression ignition (HCCI) engines. In: Proceedings of the 47th IEEE conference on decision and control, Cancun, Mexico; 2008.

[5] Chiang CJ, Stefanopoulou AG. Stability analysis in homogeneous charge compression ignition HCCI engines with high dilution. IEEE Trans Control Syst Technol 2007;15:209219.

[6] Shaver GM, Roelle MJ, Gerdes JC. Modeling cycle to cycle dynamics and mode transition in HCCI engines with variable valve actuation. Control Eng Pract 2006;14:213222.

[7] Widd A, Liao H, Gerdes J, Tunestål P, Johansson R. Control of exhaust recompression HCCI using hybrid model predictive control. In: American control conference, San Francisco, CA, USA; 2011.

[8] Shahbakhti M, Ghazimirsaied A, Koch CR. Experimental study of exhaust temperature variation in an HCCI engine. IMechE Part D: J Automob Eng 2010;224(9):1177–97.

[9] Kang JM. Sensitivity analysis of auto-ignited combustion in HCCI engines. SAE paper no. 2010-01-0573; 2010.

[10] Shahbakhti M, Lupul R, Koch CR. Predicting HCCI auto ignition timing by extending a modied knock-integral method. SAE paper no. 2007-01-0222; 2007.

[11] Kirchen PN, Shahbahkti M, Koch CR. A skeletal kinetic mechanism for PRF combustion in HCCI engines. Combus Sci Technol 2007;179:1059–83.

[12] Burcat A. Third millenium ideal gas and condensed phase thermo- chemical database for combustion. Technical report no. TAE 867. Faculty of Aerospace Engineering, Israel Institute of Technology; 2001.

[13] Heywood JB. Internal combustion engine fundamentals. New York: McGraw-Hill; 1988.

[14] Chang J, Guralp O, Filipi Z, Assanis D, Kuo T, Najt P, et al. New heat transfer correlation for an HCCI engine derived from measurements of instantaneous surface heat flux. SAE paper no. 2004-01-2996; 2004.

[15] Shahbakhti M, Koch CR. Thermo-kinetic combustion modeling of an HCCI engine to analyze ignition timing for control applications. In: Proceeding of combustion institute/canadian section (CI/CS) spring technical conference; 2007.

[16] Shahbakhti M, Koch CR. Physics based control oriented model for HCCI combustion timing. J Dynam Syst Measure Control 2010;132:021010-1 [ASME paper].

[17] Karagiorgis S, Collings N, Glover K, Coghlan N, Petridis A. Residual gas fraction measurement and estimation on a homogeneous charge compression ignition engine utilizing the negative valve overlap strategy. SAE paper no. 2006-01-3276; 2006.

[18] Cavina N, Siviero C, Suglia C. Residual gas fraction estimation: application to a GDI engine with variable valve timing and EGR. SAE paper no. 2004-01-2943; 2004.

[19] Zhao H. HCCI and CAI engines for the automotive industry. Woodhead Publishing Ltd.; 2007.

[20] Swan K, Shahbakhti M, Koch CR. Predicting start of combustion using a modied knock integral method for an HCCI engine. SAE paper no. 2006-01-1086; 2006.

[21] Chiang CJ, Stefanopoulou AG. Dynamic modeling of combustion and gas exchange processes for controlled auto-ignition engines. In: Proceeding of the 2006 American control conference; 2006.

[22] Shahbakhti M. Modeling and experimental study of an HCCI engine for combustion timing control. Ph.D. thesis, University of Alberta, fall; 2009.

[23] Vibe I. Bennverlauf und Kreisprozeβ von Verbrennungsmotoren (in German), VEB Verlag Tecknik, Berlin Germany; 1970.

[24] Shahbakhti M, Koch CR. Control oriented modeling of combustion phasing for an HCCI engine. In: Proceeding of 2007 American control conference, New York, USA, July 11–13; 2007. p. 3694–99.

[25] Shahbakhti M, Koch CR. Characterizing the cyclic variability of ignition timing in an HCCI engine fueled with n-Heptane/iso-Octane blend fuels. Int J Eng Res 2008;9(5):361–97.

[26] Turns SR. An introduction to combustion: concepts and applications. 2nd ed. New York: McGraw-Hill; 2000.